Additive Manufactured and Topology Optimized Flexpin for Planetary Gears

Anton Höller[1(✉)], Frank Huber[1], Livia Zumofen[1],
Andreas Kirchheim[1], Hanspeter Dinner[2], and Hans-Jörg Dennig[1]

[1] Zurich University of Applied Sciences – School of Engineering – Centre
for Product and Process Development, Winterthur, Switzerland
`anton.hoeller@zhaw.ch`
[2] KISSsoft AG, Bubikon, Switzerland

Abstract. This paper shows how the interdisciplinary use of additive manu-
facturing (AM) and topology optimization (TO) lead to a better load distribution and a related increase in performance within a planetary gearbox. For this, it has been investigated how to use TO for designing the flexible support of the planets pin and to reduce thereby the load sharing factor ($K\gamma$). 18 digital experiments were performed to evaluate the best setting for this TO. A completely new shape for a "flexpin" design was found which offers significant advantages in terms of compliance and misalignment for the flexible support structure of planet gears. Because of AM, the focus can stay on the main function of the flexpin including the component reduction. Critical interfaces are no longer necessary. This allows a much better definition of the compliance, an improved assembling, and a safer operation. The best TO-design concept was selected and edited for additive manufacturing. The final validation by FEM showed an increase in load capacity by 13% and an additional reduction of the misalignment of 77%.

Keywords: Additive manufacturing · Structural optimization · Flexpin · Load distribution · Planetary gearbox

AQ1

AQ2

1 Introduction

Additive manufacturing (AM) processes such as Laser Powder Bed Fusion (LPBF) open up unique possibilities in the design and manufacture of mechanical components. Due to the layer-wise build-up of the generative manufacturing processes, structures are possible which cannot be produced by any other manufacturing process, or only at enormous effort and expense. This enables the component function to be brought much more into focus during design [1]. The popularity of additive manufacturing processes is also seen in the sales growth of the 3D printing and additive manufacturing industry. In the period from 2014 to 2019, revenue was more than doubled [2]. The possibilities of the new design freedoms for components have been presented in various scientific papers [3–5]. In order to achieve economical solutions for additively manufactured mass-production components, an additional functional integration must also be targeted in addition to the production-oriented redesign.

These novel design freedoms through additive manufacturing offer the possibility to better fit the topology of the component to the requirements within its application. This paper investigates the possibilities of AM by use of TO for an improved design of the flexpin within a planetary gear train.

By using planetary gears, large transmission ratios can be achieved in a space-saving manner, with high efficiency and comparatively low self-weight. Planetary gears have a very wide range of applications in industry, automotive engineering, aerospace, and aviation.

Due to the arrangement of the planet gears, special attention must be paid to the load distribution among the planets. Manufacturing and assembly tolerances lead to uneven load distribution to the planet gears. This is considered by the load distribution factor $K\gamma$ as used in gear rating along e.g. ISO 6336. It is known that a significantly better load distribution can be achieved by a specific compliant design of the planet supports, often also called flexpin [6]. There are different geometrical shapes of the flexpins. However, so far only the possibilities of subtractive manufacturing were considered during the development. Thereby a notched pin is usually inserted into the planet carrier, which in turn carries a sleeve at the other end [7]. Thus the flexpin is usually built up from three individual parts, which are often press-fitted, Fig. 1.
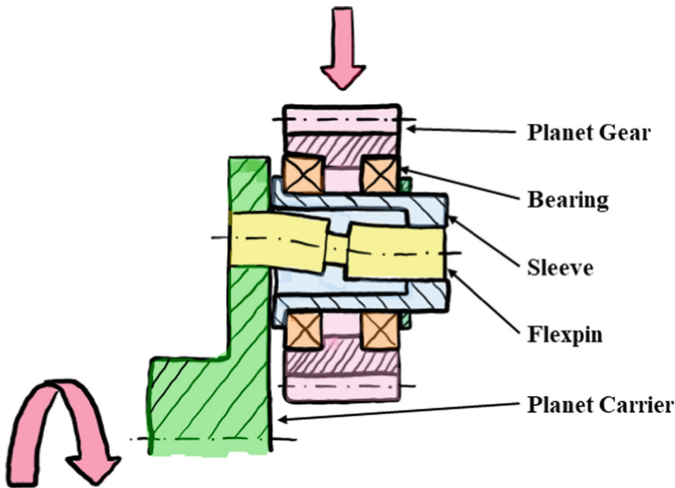

Fig. 1. A common design of flexpin

2   State of the Art

2.1   Planetary Gear Trains

Gears are used in mechanical engineering where rotational speed and torque must be converted. A common type of gearbox is the planetary gearbox. Thereby the central wheel (sun) drives one or more rotating gear wheels (planets). A ring gear with internal teeth encloses the planets. The planets are usually evenly distributed around the

perimeter. They are linked by the planet carrier. In the basic operating mode, the sun (Fig. 2, 1) drives the planets (Fig. 2, p), which are coupled to the output shaft through the planet carrier (Fig. 2, s). The ring gear (Fig. 2, 2) remains stationary and is fixed to the housing.
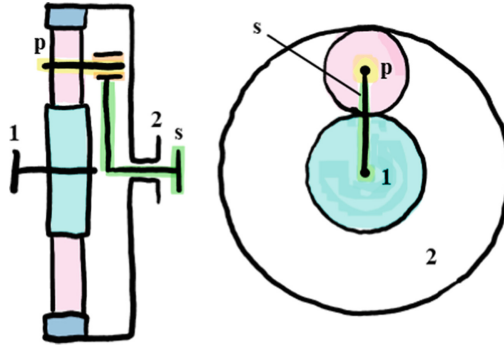
Fig. 2. Planetary gear train (1: Sun gear, 2: Ring gear, p: Planet gear, s: Planet carrier) [8]

With planetary gear trains, large transmission ratios can be achieved in a space-saving manner, with comparatively low dead weight and low moments of inertia [6, 8]. This leads to higher efficiencies and increased power densities. The compact design also raises certain challenges. Thus, planetary gears impose higher demands on the manufacturing accuracy. Furthermore, when using two or more planetary gears, the system is statically overdetermined.

A number of different standards and methods are known for the dimensioning of gears made of steel. Well established are ISO 6336:2006 method B, DIN 3990 method B and AGMA 2001-C95. For this work, the calculations were made according to ISO 6336. The fail-safe design of gearboxes has to take several different influencing factors into account, which are mainly selected according to the design and application of the gearbox. The load sharing factor K_γ and the face load factor $K_{H\beta}$ represent two main factors in the sizing process [9]. The load sharing factor K_γ considers the uneven load distribution from the sun to the planets. With the face load factor $K_{H\beta}$ the uneven load distribution over the tooth width can be taken into account. In accordance with [10], the load sharing factor is defined as follows:

$$K_\gamma = \frac{F_{timax}}{F_t} > 1, \tag{1}$$

K_γ: Load Sharing Factor
$F_{ti\ max}$: Maximum Tangential Force for Planet i of n
F_t: Nominal Tangential Force

In accordance with [10], the face load factor is defined as the maximum load intensity compared to the average load intensity:

$$K_{H\beta} = \frac{(F_{tj}/b_j)_{max}}{(F_{tm}/b)} > 1, \tag{2}$$

$K_{H\beta}$: Face Load Factor
F_{tj}: Amount of Tooth Force in Section b_j
b_j: Section of the Tooth Width
F_{tm}: Average Tooth Force
b: Tooth Width

Furthermore, the internal dynamic factor (K_V) enables the additional torque caused by the tooth quality, speed and load to be considered [10]. The application factor (K_A) additionally increases the nominal load additionally. These additional loads depend on the characteristics of driving and driven machines as well as on the mass and stiffness of the system. The factors K_A and K_V are given by the application and cannot be influenced by the design of the planetary mounting. Therefore, they are no further relevant for this work.

The tangential force is used in several cases during design. Thus, in addition to the stress in the planet pin, it is also crucial for the stress in the tooth root and the tooth flank of the gears as well as for the dimensioning of the planet bearings [10].

For single-stage planetary gearboxes (Fig. 2) the nominal tangential force F_t, acting on the planet axis, can be calculated based on the nominal output torque (M_n):

$$F_t = \frac{M_n}{n_P \cdot r_P} \tag{3}$$

M_n: Output Torque
n_P: Number of Planets
r_P: Effective Radius of Planetary Axis

The dimensioning tangential force F_t' on the planet can be calculated according to Eq. 3 [10]:

$$F_t' = F_t \, K_A \, K_V \, K_{H\beta} \, K_\gamma, \tag{4}$$

Unavoidable manufacturing or assembly inaccuracies always lead to an uneven load sharing among the planet gears. It could be shown that an improved load sharing can be achieved by a specific compliant design of the supporting structure of the gearing components [6]. The improved load sharing is achieved by deformations caused by the operating load being significantly larger than the manufacturing inaccuracies to be compensated. One solution is the flexible design of the planetary support structure. Therefore, Raymond Hicks patented the flexpin design in 1967 [11]. Hicks placed the planetary bearings on a sleeve, which generates a counter torque under load due to its one-sided attachment to the pin. This design concept allows parallel displacement of the gear wheel under load with additional flexibility. In 2006 Fox and

Jallet extended Hicks' idea with an additional notch in the pin, which further reduces the stiffness [7]. The following are named as negative influencing factors for load sharing [6]: Eccentricity of the gears, position deviation of the planet pin bore in the carrier and uneven radial clearance distribution of the planet bearings. As positive influences, Arnaudov names the flexibility of the transmission elements as well as radial bearing clearance of the central shafts (of sun and carrier). It was also found that the load distribution depends on the torque, the bearing clearance and the number of planets. Based on Kahraman's research, Montestruc investigated the load distribution in planetary gears numerically [12, 13]. The developed model considers the three most influential errors: the position error of the planet pin and the errors caused by the tooth thickness tolerance and the runout of the gear. Montestruc [13] concludes that the flex pin has a positive effect on the load sharing, even with a higher number of planets (up to 11), the reduction of stiffness also reduces the resonance frequency and the load sharing depends on the load case. In order to represent the compliance comprehensively, the stiffness of the component interfaces, the carrier, the roller bearings and the tooth contacts must be considered in addition to the compliance of the flexpin [6, 14].

A scientific study on the shape of the flexpin has not been found. Dinner analyses different forms of notches. He concludes that the notch in the shape of a double cone offers the best compromise between compliance and stress. Further, he points out that the position of the notch is usually force-symmetrical in order to reduce a misalignment of the gear [9].

Neubauer and Dinner show the relevance of the stiffness of the interfaces. [9, 14] The component interfaces are also crucial for an exact design of the elasticity of the planet pin. There has been no scientific investigation found for this problem in the design of the flexpin.

2.2 Topology Optimization

AM offers completely new possibilities for lightweight designs. Both Emmelmann and Brackett state that AM is redefining lightweight design, especially for aviation applications [15, 16]. Plocher offers a comprehensive report on the state of research and industry. He shows, among other aspects, various approaches to lightweight construction through topology optimization (TO) [17]. The TO has been significantly further improved in recent years [15, 18].

A common TO approach is Solid Isotropic Material with Penalization (SIMP), which is also applied by the software used in this study. Thereby the design space is divided into small areas, the design variables x (DV). A relative material density ($\rho_{ne}(x)$) is assigned to each DV, which is used to optimize the component. The material density can adopt values between 0 (void) and 1 (solid). Starting from a FEM calculation, new design proposals are generated by the TO. The specifications such as maximum design space, deformations, loads, remaining volume and compliance for a defined target function are fulfilled in an optimum manner [15, 19]. In a simple TO, the mean compliance is minimized while maintaining a weight restriction. In TO, manufacturing restrictions such as the maximum overhang angle for a given print direction, component symmetries, direction of demolding can be introduced by constraints [18, 20].

The generated design concepts are non-parametric models and need to be processed for further use after optimization. Therefore, the obtained density distribution of the DV must be interpreted and converted into a component by a Computer Aided Design (CAD) program [19].

2.3   Additive Manufacturing in the Context of Gear Components

Thanks to the layer-wise build-up of components and the subsequent possibilities, AM is called a disruptive technology for manufacturing [21]. The research in the field of AM has made significant achievements in recent years. Thus, more complex components with higher mechanical requirements can be additively produced. Thanks to the layer-wise structure of additive manufacturing processes, structures are possible which cannot be produced by other manufacturing processes, or only at great expense. This enables the component function to be brought much more into focus during design [1]. For mechanically highly loaded metal components, the Laser Power Bed Fusion (LPBF) process is of major relevance.

Rogers shows the potential for the gear industry through AM [21]. He identifies several fields of action: Production of complex geometries such as internal cooling and lubrication channels, reduction of mass inertia, improvement of fatigue strength, reduction of manufacturing costs, reduction of development and time to market. The number of studies that explore the design potential of AM and TO in gear train design is limited. Kamps has developed a new method to develop an innovative gear design which can be manufactured by AM [22]. Ramadani calculated a vibration- and weight-optimized gear made of Ti-6Al-4 V by LPBF [23]. Thereby he uses lattice structures to reduce noise emissions. Barreiro analyzes the potential and the restrictions due to AM using the example of a transmission housing TO [24]. He highlights the importance of integrating additional functions, such as lubrication channels.

Focused on AM and TO, the potential of AM in combination with TO has already been investigated in several scientific studies. [18, 25–30] Almost all designs were topology optimized in terms of stiffness at mass constraint. Scientific research in terms of Gearbox Development and TO, has also been accomplished many times [21, 32–36]. Kolakowski [32] for example has optimized a planet carrier with the aim of improving torsional stiffness. Jeevanantham [35], Zhuang [34] and Dietzel [37] developed new gearbox cases. Some authors [36, 38, 39] address the topic of the optimal shape of a gear wheel. Both Shah [38] and Heiselbetz [36] reduce the weight with respect to symmetry and stress constraints. Furthermore, also the modal behavior was investigated [36]. TO has been successfully used in the development of gear trains and has improved some components. However, no paper has been found about the flexible support of the planets by using TO nor AM.

3   Development Process and Methodology

The present work has the goal of an optimized flexpin design, which uses the freedom of AM for better performance. Therefore, a reference gearbox was defined (Fig. 3, No. 1). To obtain the load distribution, a simplified static FEM model of the gearbox

was created alike the model by Montestruc [13]. This model contains the influences of tangential differences in clearance at the tooth contact of the planets and thus makes it possible to show the load-dependent load sharing for this gearbox. With this model, the load distribution was analyzed, the potential for increased compliance of the planetary support was demonstrated and a target stiffness value was defined (Fig. 3, No. 2). Using a submodel, the structure of the planetary pin was optimized in such a way that the stiffness specification is met but the tilting of the sleeve is minimized and the stress on the pin remains within the allowable limits. The static qualification was performed against yielding with a safety factor $S_F = 2.0$ (Fig. 3, No. 3). After successful optimization, the results were transferred to a design suitable for AM (Fig. 3, No. 4) Finally, a final validation of the solution by a FEM calculation and qualitative comparison of the new solution to the existing flex pin design has been carried out. It was clarified whether further performance increases are possible thanks to the use of AM.
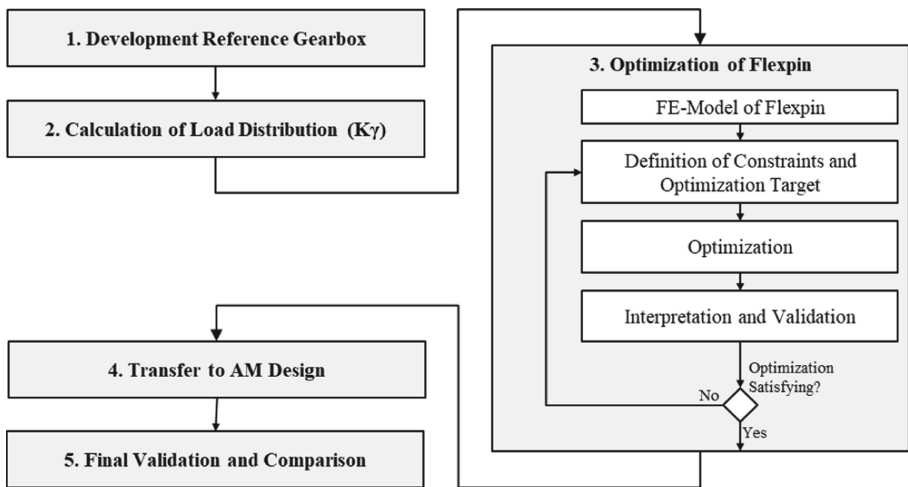

Fig. 3. Development process

The planetary gear was designed with the KISSsys 2019a, by KISSsoft. For the FEM calculations ANSYS 2019 R3 has been used and for the optimization Tosca Structure 2018 (Hotfix 5) from Dassault Systems has been used.

3.1 Development of Reference Gear Train

The starting point is a newly developed reference gear train with a total ratio of 4.33:1 and a nominal power of 60 kW (Fig. 4). The output shaft has a rotational speed of 1'200 rpm at a torque of 477.5 Nm. The drive shaft is connected by bolts to the sun wheel. The five planet wheels are placed in a regular 72° pitch. They are supported by needle bearings through a hollow pin and a sleeve in the planet carrier (Fig. 5). The planet pins are only one sided supported in the planet carrier. The planet carrier is connected by bolts to the

output shaft. The output shaft is bearing mounted in the housing. The normal module of the spur gearing is 1.5 mm. All structural components are made by titanium (Ti-6Al-4 V) and all gears made of case-hardening steel (16MnCr5). Further information about the gearing can be found in the following table (Table 1).
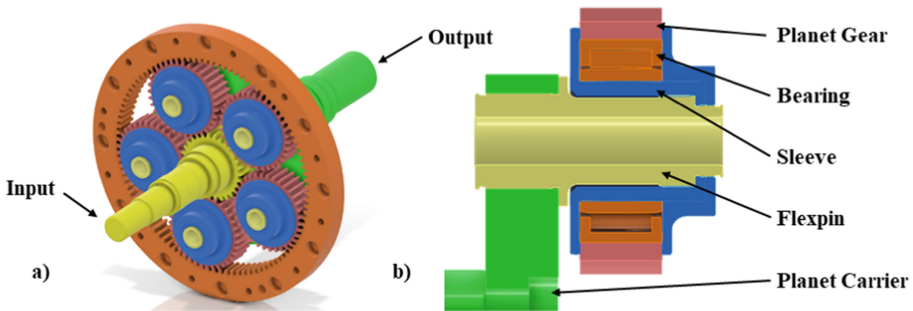
Fig. 4. Reference gear train (a: Isometric view with hidden gear box, b: Section view of planet gear)

Table 1. Most important gearing data of the reference gear

			Sun Gear	Planet Gears	Ring Gear
Normal module	m_n	mm	1.5	1.5	1.5
Pressure angle at normal section	α_n	°	20	20	20
Quality[a]	Q	–	6	6	6
Tooth width	b	mm	17	17	15
Pitch circle diameter	d	mm	45	52.5	150
Addendum modification coefficient	x		0	0	0

[a] According ISO1328:1995.

   The planet gears (Fig. 4b) are mounted on the sleeve with needle bearing SKF NA 4905 and are guided by lateral stops. The sleeve is press-fitted onto the and additionally secured by a circlip (not shown). The pin is press-fitted into the planet carrier.

## 3.2   Calculation of Load Distribution

In order to calculate the load sharing in the reference gear, it is crucial to combine the stiffness of the five flexpin assemblies (all five assemblies have the same stiffness) with the different backlashes in the gear meshes (backlashes between the five planet gears and the mating gears are not the same for all five planets due to manufacturing errors). A FEM model (Fig. 5) was developed, which shows the stiffness along the force flow from the sun to the output shaft, over the planet carrier, planet pin, sleeve by finite elements. The radial bearing stiffness and the bearing clearance of the planetary bearings are implemented in the calculation by spring elements with gap option. The bearings of

the input and output shaft are assumed to be clearance-free. The tooth contact stiffness for the contacts between sun to planets and planets to ring gear is also implemented using spring elements with a constant value according to ISO 6336.

For the analysis, three errors for different tooth contacts were considered. [6, 12] These are the different radial bearing clearances limited by the bearing clearance tolerances, the radial position of the finished flexpin sleeves and the pitch deviation of the toothing of the planet gears determined by the gear quality. SKF specifies a tolerance width of 25 µm for the internal clearance for the bearings selected. [40] The positioning accuracy of the flexpin axis with respect to the gearbox axis is assumed to be ±10 µm due to IT6. The gear tooth to tooth pitch deviation of 7 µm follows from Q-ISO1328:1995 and gear quality Q6. For the calculation, the most conservative combination has been considered. This results when the tolerances for one planet gear are at the minimal level and the tolerances for all other planet gears are at the maximal level [13].

In accordance with ISO/TS 16281, KISSsoft 2019 calculates the radial stiffness of the journal rolling element bearings at the operating point with 438'560 N/mm and the tooth contact spring stiffness according to ISO 6336 with 52'346 N/mm.
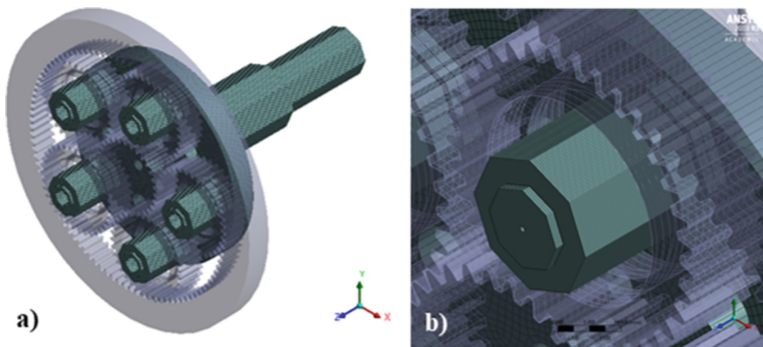

Fig. 5. FEM model of reference gear train (a: Isometric view, b: Detail view of planet gear and flexpin)

If a real gear train is loaded, at small loads one planet transmits the complete torque, due to the uneven load distribution. For a gearbox with n planets this results in a $K\gamma = n$. Due to the compliance of the loaded components the load distribution is further improved by increasing torque. This is coherent with the results of [6, 12, 14, 31] (Fig. 6). By use of the FEM Model and an applied nominal torque M_n a maximum tangential force $F'_{t,max}$ of 2791.4 N, the nominal tangential force follows from (1) with F_t of 1956.92 N and therefore $K\gamma$:

$$K_\gamma = \frac{2791.4N}{1956.9N} = 1.43,$$
(5)

The flexpin provides primarily additional tangential compliance. Behavior with flexpin is investigated using an increased overall compliance C_R, as the sum of radial bearing stiffness and radial flexpin stiffness. As expected, this resulted in a better load distribution.
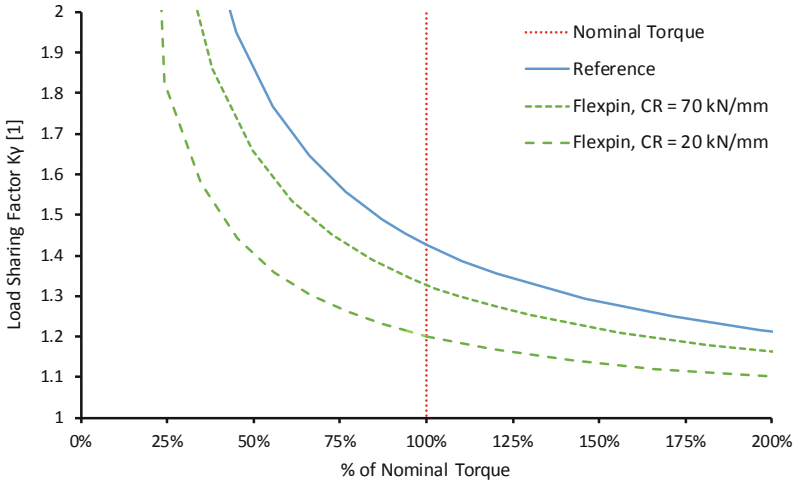
Fig. 6. Mesh load factor for reference gear train

For different radial stiffness C_R the improved load distribution can be computed (Table 2). For the optimization, the target stiffness of the flexpin is assumed to be $C_R =$ 20 kN/mm. At a constant tangential load, (3) follows a potential increase in torque of 19%.

Table 2. Load sharing factor for different radial stiffness

Radial Stiffness C_R [kN/mm]	Load Sharing Factor $K\gamma$ [-]
6	1.095
15	1.170
20	1.200
30	1.245
70	1.330

4 Results and Discussion

4.1 Topology Optimization of Flexpin

For the TO of the flexpin, a reduced model was created. It contains the essential geometric elements to represent the force flow over the flexpin. A coordinate system C0 was defined (Fig. 7, No. 2). The central axis of the flexpin is coincident with the Z-axis. From Fig. 6 with M_n and $C_R = 20$ kN/mm follows $K\gamma = 1.2$. This leads to a maximum tangential force per flex pin of $F'_{t,max} \approx 2'300$ N. It is applied to the contact surfaces of the planetary bearing (Fig. 7, No. 3). The material behavior was assumed to be linear-isotropic. For the LPBF manufactured Ti-6Al-4 V an elastic modulus of 115 GPa was defined [41].
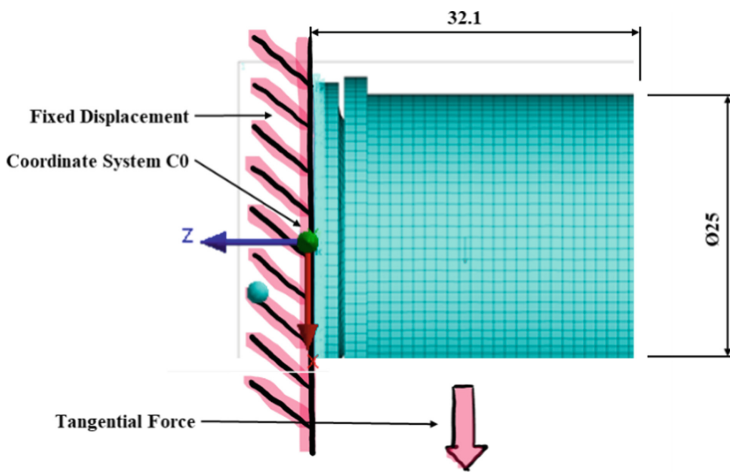
Fig. 7. Basis model for the TO of the flexpin

Two primary criteria are defined for the application of the flexpin: the local radial stiffness C_R for the flexpin, for a defined load distribution and the minimum misalignment α of the sleeve, which leads to an uneven load distribution across the width. For the TO an additional node N is defined at the position (-100/0/-13). The radial stiffness of the solution is derived from the deformation of node N in X-direction u_{xN}. The tilting of the sleeve corresponds to a rotation around the Y-axis. This is measured by the axial displacement of node N u_{zN}.

The TO was performed with the target function and constraints specified in Table 3. The overhang constraint was defined with the print direction -Z and the overhang angle of 45°.

Table 3. TO of flexpin for AM

| Target Function	Minimize (uz_N)
Constraint C1	$ux_{min} < ux_N < ux_{max}$ with ux_{min} = 0.2185 mm and ux_{max} = 0.2415 mm
Constraint C2	Overhang 45°, Print Direction -Z
Constraint C3	Volume reduction = 50%
Constraint C4	SIG_TOPO_MISES[a] = 75 MPa
Constraint C5	Plane Symmetry XZ

[a] SIG_TOPO_MISES is defined by Tosca Structural [42].

To further understand the influence of the constraints C2 and C3, 18 digital TO experiments are defined (Table 4). The design concepts must be processed for evaluation. For this purpose, the density distribution must be interpreted using a limit value ISO, which represents the hard border between void (no material present) and solid (material present). This is done with the program Tosca Smooth. Space Claim was used to refine the CAD geometry. The qualification of the prepared design concepts was accomplished on the criteria of radial stiffness C_{Reff}, maximum equivalent stress according to von Mises S_{vM} and the misalignment α of the bearing surfaces on the sleeve by a subsequent simulation. The allowable equivalent stress was determined on the basis of the yield stress (stress relieved, 1 h at 650 °C in vacuum) [41] and S_F to S_{allow} = 542.8 MPa.

Table 4. Overview of TO experiments

| No.	C3		C4		ISO	C_{Reff}	S_{vM}	α
	[-]		[MPa]		[-]	[kN/mm]	[MPa]	%
1	$\geq$	0.30	$\geq$	50	0.75	47.9	422.0	0.02%
2	$\geq$	0.50	$\geq$	25	0.75	108.6	151.0	−0.02%
3	$\geq$	0.50	$\geq$	25	0.90	79.4	214.5	0.00%
4	$\geq$	0.50	$\geq$	50	0.60	70.5	247.3	−0.02%
5	$\geq$	0.50	$\geq$	50	0.75	31.0	440.0	0.07%
6	$\geq$	0.50	$\geq$	50	0.78	25.1	569.4	0.14%
7	$\geq$	0.50	$\geq$	50	0.83	15.8	901.5	0.28%
8	$\geq$	0.50	$\geq$	50	0.90	6.1	1925.5	0.94%
9	$\geq$	0.50	$\geq$	75	0.70	33.4	553.9	0.01%
10	$\geq$	0.50	$\geq$	75	0.75	22.1	724.4	0.06%
11	$\geq$	0.50	n. a.		0.50	22.8	732.6	−0.05%
12	$\geq$	0.50	n. a.		0.75	5.0	2661.1	−0.15%
13	$\geq$	0.65	$\geq$	50	0.75	41.7	494.4	0.03%
14	$\geq$	0.70	$\geq$	50	0.60	76.6	283.1	−0.02%
15	$\geq$	0.70	$\geq$	50	0.75	39.7	469.0	0.04%
16	$\geq$	0.70	$\geq$	50	0.80	27.5	643.0	0.09%
17	$\geq$	0.70	$\geq$	50	0.85	13.5	1164.0	0.30%
18	$\geq$	0.70	$\geq$	50	0.90	4.1	5308.4	1.49%

Almost all design concepts are found with a design similar to a parallelogram, whereby four of each are connected by a crossbar (Fig. 8b, 8c and 8d). The form is comprehensible due to the given boundary conditions.

The cross-section of the flexural joints is strongly dependent on C3 and ISO, which therefore have a significant influence on the stiffness (Fig. 8b, Fig. 8d). The desired compliance cannot be obtained directly but must be approximated iteratively. C4 limits the maximum stress, there is a positive effect on the result, but the influence seems to be subordinate compared to other constraints. With a low value of C4 a design, like the known flexpin can be achieved. The volume and the plane symmetry constraint lead to a two "leave spring" design (Fig. 8a).
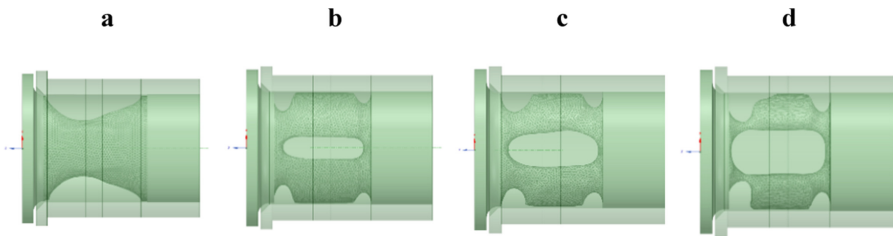
Fig. 8. Results of topology optimized flexpin, a. Design concept 3, b. Design concept 13, c. Design concept 10, d. Design concept 18

The influence of the manufacturing restrictions (C2) is getting more and more lost during processing as a result of the dense design. The overhang angle does not go directly into the processing and must be considered in the subsequent finishing in CAD manually.
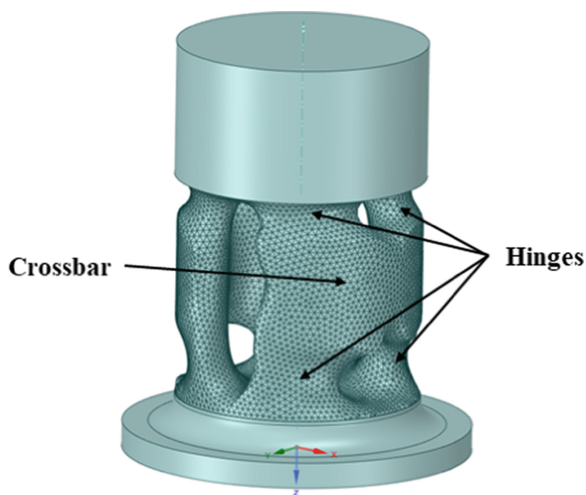
Fig. 9. Flexpin design (No. 9) after TO

No. 5, No. 9, No. 13 and No. 15 from Table 4 show a good balance between stress, compliance and misalignment. The configuration of experiment 9 is selected for further use (Fig. 9).

4.2 AM Design and Final Validation

In order to prepare the received design concept for production by LPBF, the geometry must be edited considering the following aspects:

Smoothing. The structure which is available as output of the TO must be further improved. The CAD tool Space Claim is used for this purpose. Further imperfections in the geometry will be removed. Finally, it has to be taken care that the free form surfaces are smoothed with a high resolution.

Merge the volumes. The pin and the sleeve can be merged. Special attention must be paid to the sharp transition zone of the components.

Overhang. For overhanging structures in Ti-6Al-4 V, the surface roughness increases significantly at an angle of < 40° to the horizontal [43], which was taken into account in the component design. To ensure process reliability, overhanging structures at a critical angle of 30° to the horizontal should be avoided [43, 44]. Horizontally overhanging structures up to 1 mm wide and horizontally aligned holes up to 12 mm in diameter can be produced without support structures [43]. These factors have been considered in the component design, resulting in a geometry that can be reliably manufactured with LPBF.

Gap. In order to avoid undesired melting or sintering, it must be ensured that adjacent component walls have a minimum gap of > 0.2 mm [43, 44].

Interface. The interface contour to the planet carrier was adapted regarding a down-stream test series.

Post-processing. During processing by LPBF, thermally induced internal stresses are introduced. These must be released again by suitable heat treatment (stress relieving). All functional surfaces must be machined after printing. Appropriate oversizing of the functional surfaces has been taken into account. Furthermore, the powder extraction after printing must be possible. Supports are required between the interface to the planet carrier and the sleeve. These also give additional support to the sleeve during the post-processing of the bearing surfaces. As a last step, the supports must be removed by a side milling cutter all around the circumference (Fig. 10).
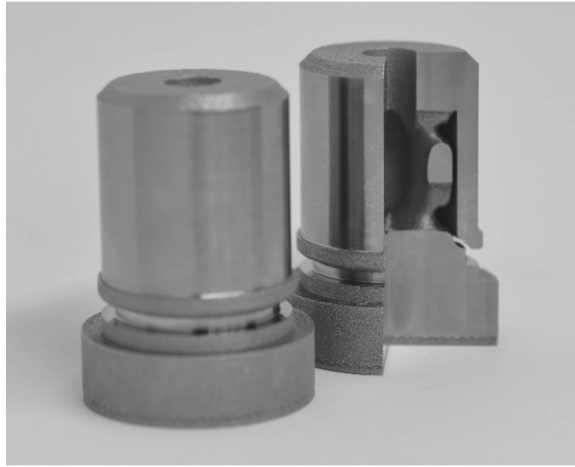
Fig. 10. Printed samples of flexpin

The solution was subjected to a FE calculation in the post-processed state. The operating tangential load F_t' must be recalculated according to (4) by the load distribution factor and the radial stiffness. The new design will reduce $K\gamma$ from 1.43 to 1.24, the fewer misalignment leads according to a first estimation by use of KISSsoft to a $K_{H\beta}$ reduction from 2.03 to 1.29. The total deformation is shown in Fig. 11 and Fig. 12 and the displacement in x direction of the path on top of the sleeve shown in Fig. 13 illustrate the reduced stiffness behavior and the improved misalignment for the load of 2'300 N of the non-optimized (Full Cross Section Design) and the optimized (AM & TO Design) flexpin. As a result of the lower stiffness, the optimized flexpin will improve the equalization of the load distribution in planetary gears. Furthermore, its reduced misalignment of the sleeve will improve the load distribution over the tooth width.
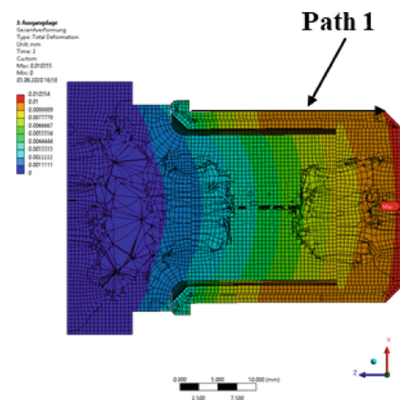
Fig. 11. Total deformation of full cross section design
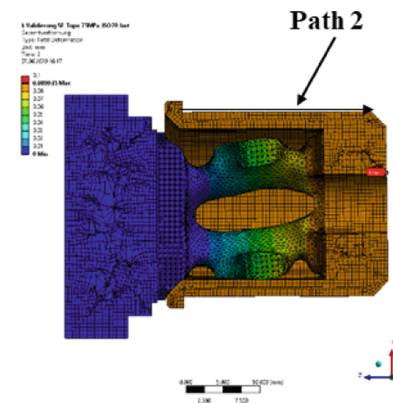
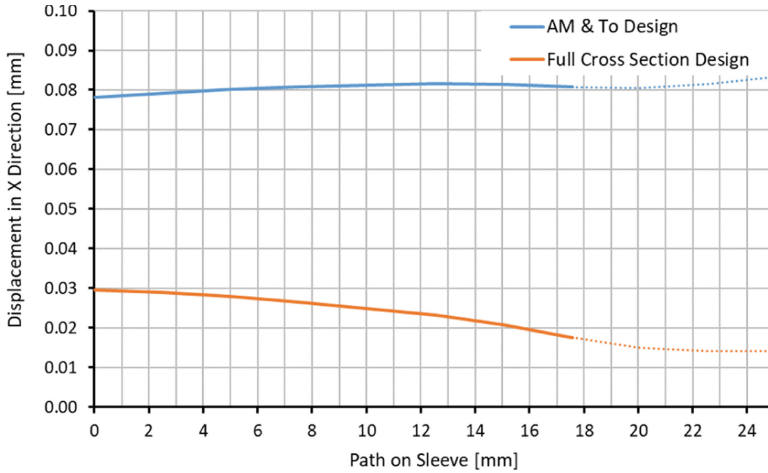**Fig. 12.** Total deformation of AM & TO design

Fig. 13. Displacement in X direction of Path 1 and Path 2 on sleeve

The structural stresses increase but stay at an acceptable level for static loads. For the optimized structure, a maximal value of 494.7 MPa for Von Mises stress was calculated (Fig. 14). The development of new flexpin requires TO. A heat treatment (stress relieving) is for the printed version mandatory. A suitable surface finishing method may positively influence fatigue properties, despite the initial high surface roughness. However, due to the entangled shape of the TO flexpin, the accessibility of the relevant surface area is limited. Therefore, primarily flow grinding is potentially applicable.
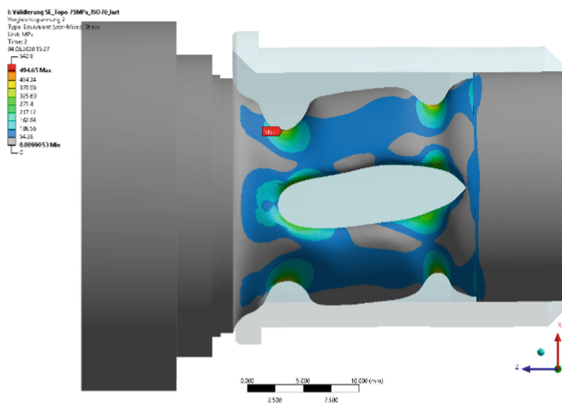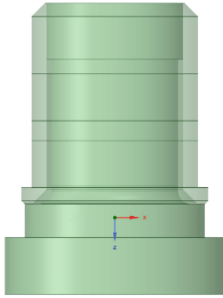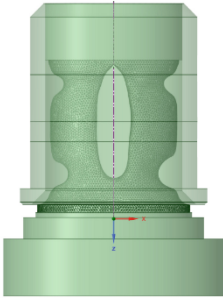


Fig. 14. Von Mises stress of AM & TO design

The comparison in Table 5 between non-optimized (Fig. 15) and optimized (Fig. 16) pin provides an overview of the added value, but also the drawbacks of the new solution.

Table 5. Comparison of Full Cross Section Design and Optimized Pin

	Full Cross Section Design	**AM & TO Design**
	Fig. 15. Pin without Flexpin	Fig. 16. Pin with AM and TO Design
Design Load for Pin	$F_t'\,(C_R, M_n) = 2'915.8$ N	$F_t'\,(C_R, M_n) = 2'421.7$ N (-17%)
Result of Simulation	• $C_R = 117.6$ kN/mm • $S_{vM} = 145$ MPa • $\lvert\alpha\rvert = 0.068\%$	• $C_R = 28.7$ kN/mm (-75.6%) • $S_{vM} = 494.7$ MPa (+341%) • $\lvert\alpha\rvert = 0.016\%$ (-77.3%)
Development	• Average complexity	• Increased complexity
Manufacturing	• Heat treatment optional • Post-processing of press fit faces	• Heat treatment mandatory • Post-processing (machining, perhaps flow grinding)
	• Well established procedures	• Increased precision due to part integration
Assembling	• Press fit (Pin/Sleeve)	• Lower number of parts and interfaces
Cost	• Higher effort for assembling	• Higher production cost expected for flexpin • Smaller loads could lead to smaller design and monetary savings of gear train
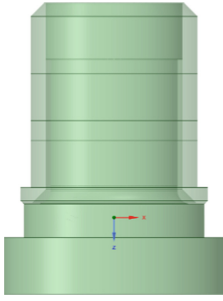
Fig. 15. Pin without flexpin
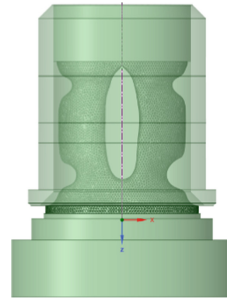
Fig. 16. Pin with AM and TO design

5   Conclusion

The present work aims at an optimized flexpin design, which uses the freedom of additive manufacturing for improved performance of a planetary gear. For this purpose, a planetary gear train was developed and analyzed regarding the uneven load sharing. On this basis, topology optimization was used to search for new solutions that take advantage of the freedom of additive manufacturing. 18 digital experiments were carried out. A new, unique approach of a 'flexible' pin was found which significantly improves the torque distribution to the planetary gears due to radial compliance. Currently, the flexpin is designed with a notched pin [7, 11]. The parallelogram-like design promises not only a significantly lower radial compliance, but also a lower misalignment of the sleeve while respecting the stress limits. The newly discovered design features an optimized geometry that takes full advantage of the AM design freedom. The stiffness can be adjusted according to the application. Thanks to the part integration of sleeve and pin, this critical interface is no longer present for the first time. This enables a more precise design, manufacturing, assembling and finally operation. The further improved load distribution allows to keep the dimensioning tangential load on the planet pins on a lower level. Due to its influence on the gear dimensioning and bearing selection, this is crucial for the costs generated in gear design. In order to ensure safe operation, an additional proof of fatigue strength must be provided in future work. Within this context, suitable surface treatments for the TO surface need to be evaluated and the accessibility of relevant surface areas needs to be addressed in future work.

The transfer from the design concept proposed by the TO to a design suitable for production offers further potential for improvement. During smoothing, valuable information of the geometry data is lost. Criteria for the overhang angle need to be considered again during the preparation of the 3D data for AM.

It is intended to use the gained knowledge to realize the flexible support of the planet as an integrated part of the planet carrier. Thanks to the elimination of the interfaces between planet carrier, pin and sleeve, the performance of the gearbox can be further improved.

References

1. Wörner, S., et al.: Rapid Prototyping im Maschinen- und Automobilbau – Ermüdungseigenschaften additiv gefertigter Bauteile in Additive Fertigung von Bauteilen und Strukturen, 1st edn. Springer, Wiesbaden (2017)
2. Wohlers, T., et al.: "Wohlers Report 2018", 3D-Printing and Additive Manufacturing State of the Industry – Annual Worldwide Progress Report. Wohlers Associates, Fort Collins/US (2018)
3. Spiegel, A., et al.: Lightweight Design: Wege zum wirtschaftlichen Einsatz der laseradditiven Fertigung. Springer, Wiesbaden (2015)
4. Grienitz, V., et al.: ATZ - Automobiltechnische Zeitschrift: Technikevaluation für die generative Fertigung eines Serien-Radträgers. Springer, Wiesbaden (2016)
5. Wartzack, S., et al.: Besonderheiten bei der Auslegung und Gestaltung lasergesinterter Bauteile, RTejournal - Forum für Rapid Technologie, vol. 7 (2010)
6. Arnaudov, K., Karaivanov, D.: Planetary Gear Trains, 1st edn. CRC Press, Boca Raton (2019)
7. Fox, G., et al.: Epicyclic Gear System, US6994651 B2, United States Patent Office (2006)
8. Wittel, H., et al.: Roloff/Matek Maschinenelemente, 24th edn. Springer, Wiesbaden (2019)
9. Dinner, H., et al.: FlexPin Design for Maximized Power Density. EES KISSSOFT GmbH, Menzingen (2014)
10. ISO 6336-1-2006: Calculation of load capacity of spur and helical gears (2006)
11. Hicks, R.J.: Load Equalizing Means for Planetary Pinions, US3303713. United States Patent Office (1967)
12. Kahraman, A.: Static Load Sharing Characteristics of Transmission Planetary Gear Sets: Model and Experiment. SAE Technical Paper 1999-01-1050 (1999)
13. Montestruc, A.: A Numerical Approach to Calculation of Load Sharing in Planetary Gear Drives. Journal of Mechanical Design, ANSI/AGMA Paper No. 6123-B06 (2009)
14. Neubauer, B.: Lastverteilung und Anregungsverhalten in Planetengetriebensystemen, Dissertation. Technischen Universität München (2016)
15. Bendsoe, M.P., et al.: Topology Optimization: Theory, Methods, and Applications. Springer, Berlin (2013)
16. Emmelmann, C., et al.: Laser additive manufacturing and bionics: redefining lightweight design. Phys. Procedia, **12**(part 1), 364–368 (2011)
17. Plocher, J., et al.: Review on design and structural optimisation in additive manufacturing: towards next-generation lightweight structures. Mater. Des. **183**, 108164 (2019)
18. Zhu, J.-H., et al.: Topology optimization in aircraft and aerospace structures design. Arch. Computat. Methods Eng. **23**, 595–622 (2016)
19. Schuhmacher, A.: Optimierung Mechanischer Strukturen, 2nd edn. Springer, Wiesbaden (2013)
20. Brackett, D., et al.: Topology optimization for additive manufacturing. Annual International Solid Freeform Fabrication Symposium. Austin (Texas) (2011)
21. Rogers, K.: Additive Manufacturing Technologies for Gears. AGMA (2019)
22. Kamps, T., et al.: Systematic biomimetic part design for additive manufacturing. In: 3rd CIRP Conference on BioManufacturing, Procedia, vol. 65, pp. 259–266. ScienceDirect (2017)
23. Ramadani, R., et al.: Topology optimization based design of lightweight and low vibration gear bodies. Int. J. Simulat. Modell. **17**(1), 92–104 (2017)
24. Barreiro, P., et al.: New improvement opportunities through applying topology optimization combined with 3D printing to the construction of gearbox housings. Forsch Ingenieurwes, vol. 83, pp. 669–681. Springer, Wiesbaden (2019)

25. Ghungarde, V., et al.: Design optimization of steering knuckle by adopting bionic design approach. IOP Conf. Ser.: Mater. Sci. Eng. 624, 012023 (2019)
26. Ohlsen, J., et al.: ATZ - Automobiltechnische Zeitschrift: Function Integrated. Bionic Optimised Vehicle Lightweight Structure in Flexible Production. Springer, Wiesbaden (2015)
27. Seabra, M., et al.: Selective laser melting (SLM) and topology optimization for lighter aerospace components. In: Conference 15th PCF, Procedia Structural Integrity, vol. 1, pp. 289–296. Paço de Arcos (2016)
28. Sugavaneswaran, M., et al.: Design of robot gripper with topology optimization and its fabrication using additive manufacturing. In: Shunmugam, M.S. (ed.) Advances in Additive Manufacturing and Joining 2018. Springer, Wiesbaden (2020)
29. Smith, C.J., et al: Utilizing additive manufacturing techniques to fabricate weight optimized components designed using structural optimization methods. Solid Free. Fabr. Symp. 879–894 (2013)
30. Morgen, D., et al.: GE jet engine bracket challenge: a case study in sustainable design. J. Innov. Impact 7, 95–107 (2016)
31. Yi, P., et al.: The multi-objective optimization of the planet carrier in wind turbine gearbox. Appl. Mech. Mater. 1662-7482, **184–185**, 565–569 (2012)
32. Kolakowski, Z.: Application of structural topology optimisation for planetary carrier design. Selected problems of continuum mechanics (2016)
33. FE-SESIGN GmbH: "Weight reduction of a planet carrier with stiffness requirements". https://support.ansys.com/staticassets/ANSYS/staticassets/partner/FEDesign/Application_TOSCA_ANSYS_Optimization%20of%20a%20Planet-Carrier.pdf. Accessed 15 Feb 2020 (2010)
34. Zhuang, S.: Gearbox housing topology optimization with respect to gear misalignment. Master Thesis. Department of Management and Engineering, Linköpings universitet (2012)
35. Jeevanantham, A.K., et al.: Topology and shape optimization of gear casing using finite element and taguchi based statistical analyses. ARPN J. Eng. Appl. Sci. **11**(23) (2016)
36. Casiello, M.: Static and Dynamic Topology Optimization for Aeronautical Gears. Master Thesis. Politecnico di Torino (2018)
37. Dietzel, M.: Topology optimization methods applied to automotive transmission housings. In: European HyperWorks Technology Conference (2011)
38. Shah, C., et al.: Optimizing weight of a gear using topology optimization. Int. J. Sci., Eng. Technol. Res. (IJSETR), **7**(6) (2018)
39. Heiselbetz, U., et al.: Weight optimization of a gear wheel considering the manufacturing process and cyclic symmetry. In: 9th Stuttgart International Symposium "Automotive and Engine Technology" (2009)
40. SKF, Table of Internal Radial Clearance for Needle Roller Bearings. https://www.skf.com/de/products/bearings-units-housings/roller-bearings/needle-roller-bearings/needle-roller-bearings-with-machined-rings/with-machined-rings-w-inner-ring/index.html. Accessed 19 02 2020
41. Fischer, M., Zumofen, L.: Tensile properties of laser melted Ti6AL4V. ZHAW/ZPP. unpublished
42. Tosca Structure User Guide. SIMULIA User Assistance 2018. Dassault Systems (2018)
43. Kranz, J.: Methodik und Richtlinien für die Konstruktion von laseradditiv gefertigten Leichtbaustrukturen, 1st edn. Springer, Berlin (2017)
44. Van Bael, S., et al.: Micro-CTbased improvement of geometrical and mechanical controllability of selective la-ser melted Ti6Al4V porous structures. Mater. Sci. Eng., A **528**(24), 7423–7431 (2011)

AQ4

Author Query Form

Please ensure you fill out your response to the queries raised below and return this form along with your corrections.

Dear Author,

During the process of typesetting your chapter, the following queries have arisen. Please check your typeset proof carefully against the queries listed below and mark the necessary changes either directly on the proof/online grid or in the 'Author's response' area provided below

Query Refs.	Details Required	Author's Response
AQ1	This is to inform you that corresponding author has been identified as per the information available in the Copyright form.	
AQ2	Please provide the valid ORCID. Amend if necessary.	
AQ3	Please check and confirm if the inserted citation of Table 1 is correct. If not, please suggest an alternate citation.	
AQ4	Please supply the page range for Reference [35 and 38].	